AD-775 235

INVERSE SCATTERING

Norbert N. Bojarski

Norbert N. Bojarski

Prepared for:

Naval Air Systems Command

February 1974

UNCLASSIFIED

SECURITY CLASSIFICATION OF THIS PAGE (When Data Entered)

AD-775 235

REPORT DOCUMENTATION PAGE		READ INSTRUCTIONS BEFORE COMPLETING FORM
1. REPORT NUMBER N00019-73-C-0312/F	2. GOVT ACCESSION NO.	3. RECIPIENT'S CATALOG NUMBER
4. TITLE (and Subtitle) INVERSE SCATTERING		5. TYPE OF REPORT & PERIOD COVERED FINAL REPORT, 1973
		6. PERFORMING ORG. REPORT NUMBER
7. AUTHOR(s) Bojarski, N. N.		8. CONTRACT OR GRANT NUMBER(s) N00019-73-C-0312
9. PERFORMING ORGANIZATION NAME AND ADDRESS Norbert N. Bojarski 16 Circle Drive Moorestown, New Jersey 08057		10. PROGRAM ELEMENT, PROJECT, TASK AREA & WORK UNIT NUMBERS
11. CONTROLLING OFFICE NAME AND ADDRESS Naval Air Systems Command ATTN. AIR-310B Washington, D. C. 20361		12. REPORT DATE February 1974
		13. NUMBER OF PAGES 20
14. MONITORING AGENCY NAME & ADDRESS (if different from Controlling Office)		15. SECURITY CLASS. (of this report) Unclassified
		15a. DECLASSIFICATION/DOWNGRADING SCHEDULE

16. DISTRIBUTION STATEMENT (of this Report)

APPROVED FOR PUBLIC RELEASE;
DISTRIBUTION UNLIMITED

17. DISTRIBUTION STATEMENT (of the abstract entered in Block 20, if different from Report)

18. SUPPLEMENTARY NOTES

19. KEY WORDS (Continue on reverse side if necessary and identify by block number)

Inverse Scattering

20. ABSTRACT (Continue on reverse side if necessary and identify by block number)

The Physical Optics and Exact Inverse Scattering Solutions of this author are summarized. For the Physical Optics Inverse Scattering Method, shown are computer-reconstructed images of a sphere and cylinder from computed synthetic scattering data, as well as a sphere from experimentaly measured data. For the Exact Inverse Scattering Method, shown are computer-reconstructed source distributions (currents) of a half-wave dipole antenna, a point-source, and two point-sources separated by one-half-wavelength, from computed synthetic scattering data.

INVERSE SCATTERING

NORBERT N. BOJARSKI

16 CIRCLE DRIVE
MOORESTOWN, NEW JERSEY 08057
(609) 235-3001

Final Report to
Contract N00019-73-C-0312

February 1974

APPROVED FOR PUBLIC RELEASE;
DISTRIBUTION UNLIMITED

DEPARTMENT OF THE NAVY
NAVAL AIR SYSTEMS COMMAND
WASHINGTON, D. C. 20360

ABSTRACT

The Physical Optics and Exact Inverse Scattering Solutions of this author are summarized. For the Physical Optics Inverse Scattering Method, shown are computer-reconstructed images of a sphere and cylinder from computed synthetic scattering data, as well as a sphere from experimentaly measured data. For the Exact Inverse Scattering Method, shown are computer-reconstructed source distributions (currents) of a half-wave dipole antenna, a point-source, and two point-sources separated by one-half-wavelength, from computed synthetic scattering data.

TABLE OF CONTENTS

LIST OF ILLUSTRATIONS

SECTION I

INTRODUCTION

This report is a continuation of the final report [1] to the preceding contract, as well as to an earlier quarterly report [2] to this contract.

The theoretical results obtained to-date where reported on in detail in the above mentioned reports, and will thus be only briefly summarized in this report. The purpose of this report is to summarize the numerico-experimental results obtained to-date.

For the Physical Optics Inverse Scattering Method, shown are computer reconstructed images of a sphere and cylinder from computed synthetic scattering data, as well as a sphere from experimentally measured data.

For the Exact Inverse Scattering Method, shown are computer reconstructed source distributions (currents) of a half-wave dipole antenna, a point source, and two point sources separated by one-half wavelength, from computed synthetic scattering data.

SECTION II

PHYSICAL OPTICS INVERSE SCATTERING

II.1. THEORETICAL RESULTS

The basic Physical Optics Inverse Scattering Identity [1], applicable to complete bandwidth and perspective (aspect angles) information, is

$$\gamma(\mathbf{x}) = \mathcal{R}e \int d^3\kappa \; e^{i\boldsymbol{\kappa}\cdot\mathbf{x}} \left[\frac{\rho(\boldsymbol{\kappa})}{\kappa^2} \right] \tag{1}$$

where $\kappa \equiv 2k$, the range and phase normalized field-cross section ρ is related to the power cross section σ by $\rho\rho^* \equiv \frac{\sigma}{4\pi}$, and the characteristic function γ of the scatterer is

$$\gamma(\mathbf{x}) \equiv \begin{cases} 1 & , \quad \mathbf{x} \in V_B \\ 0 & , \quad \mathbf{x} \in V_B \end{cases} \tag{2}$$

where V_B is the volume of the scatterer.

If the information aperture is incomplete (i.e., only finite bandwidth and/or incomplete perspective data are available), then (1) yields the following Fredholm Convolution Integral Equation of the First Kind [5]

$$\gamma(\mathbf{x}) * \mathcal{R}e \; a(\mathbf{x}) = \mathcal{R}e \int_A d^3\kappa \; e^{i\boldsymbol{\kappa}\cdot\mathbf{x}} \left[\frac{\rho(\boldsymbol{\kappa})}{\kappa^2} \right] \tag{3}$$

where $a(\mathbf{x}) \leftrightarrow A(\boldsymbol{\kappa})$, and where $A(\boldsymbol{\kappa})$ is the characteristic information function, i.e.,

$$A(\boldsymbol{\kappa}) \equiv \begin{cases} 1 \quad , & \rho(\boldsymbol{\kappa}) \text{ known} \\ 0 \quad , & \rho(\boldsymbol{\kappa}) \text{ unknown} \end{cases} \tag{4}$$

This integral equation (3) can be solved exactly numerically by a variety of existing techniques such as the matrix methods of Ritz-Galerkin [6], the associated Least Square Best Estimate method [7], ar. associated moments method of Harrington [8], the Eigen-function expansion method of Toraldo Di-Francia [9], leading to so-called super-resolution, and the k-space method of this author [10], which also leads to super-resolution (This solution will be summarized in Sect. III.1. of this report, since similar Fredholm convolut integral equations of the first kind arise in the exact inverse problem). Several closed-form solutions of (3) for apertures of specific geometry have been obtained by Lewis [11].

Since the unknown function $\gamma(\mathbf{x})$ in the integral equation (3) is not a completely arbitrary function, but a characteristic function restricted to the form (2), the following closed-form approximate solutions [12] to (3) are obtained

$$\chi(\mathbf{x}) \cong Im \int_A d^3\kappa \; e^{i\boldsymbol{\kappa}\cdot\mathbf{x}} \left[\frac{\kappa_3 \; \rho(\boldsymbol{\kappa})}{\kappa^2} \right] \tag{5}$$

$$z(x_1, x_2) \approx \int dx_3 \; x_3 \; \chi(\mathbf{x}) \tag{6}$$

where $\chi(\mathbf{x})$ is a three-dimensional resolution density function which is a measure of the location of the surface of the scatterer, and $z(x_1,x_2)$ is the geometrical function of this surface.

II.2. NUMERICO-EXPERIMENTAL RESULTS

The solution to the integral equation (3) proposed by Lewis [13] was successfully numerically tested for a sphere by this author in 1969. This test consisted of a computer implementation of a special case version of this solution, applicable only to scatterers about which only a priori knowledge of cylindrical symmetry exists. This test essentially confirms the correctness of the basic inverse scattering identity (1) and the finite aperture integral equation (3). This solution was, however, not pursued further because of its inherent practical limitations. These limitations are the lack of generality of the required k-space aperture (i.e., the required aperture is impractical for physically realizable radar systems; which is not the case with this author's solution 5 and 6), the error enhancement introduced by the process of numerical differentiation of noisy data (vis-a-vis the error reduction resulting from the process of integration of such data in solutions 5 and 6), and the unapplicability of the Fast Fourier Transform (FFT) to this solution (which is essential if large amounts of data are to be processed in reasonable time by existing computers, yielding thre-dimensional high-resolution descriptions of arbitrarily shaped scatterers about which no a priori knowledge of special geometry exists).

Solutions (5) and (6) where computer implemented with the aid of the FFT for arbitrarily shaped apertures, realizable with existing radar systems. This computer program was tested with the exact solution of Mie for scattering by a sphere, with a variety of band limited aspect angles and fractional frequency bandwidths, with the results shown in fig. 1 and 3. The ripples in fig. 1 are due to the very small three-dimensional raster of 16^3 data points for $z(x_1,x_2)$; vis-a-vis the much larger two-dimensional raster of 128^2 data poins for $\chi(x_1,x_2,0)$ in fig. 3, for which these ripples disapear. A full bandwidth three-dimensional display of a reconstructed cylinder is shown in fig. 2.

Solution (5) was also tested against experimentally measered (in unechoic chamber by The General Dynamics Corp., Fort Worth, Texas) scattering data from a test sphere; the results are shown in Fig. 4 and 5; in the latter figure the

the correct size of the sphere was added (it is this author's opinion that the small faint circular images are due to interference between the test sphere and its supporting strut).

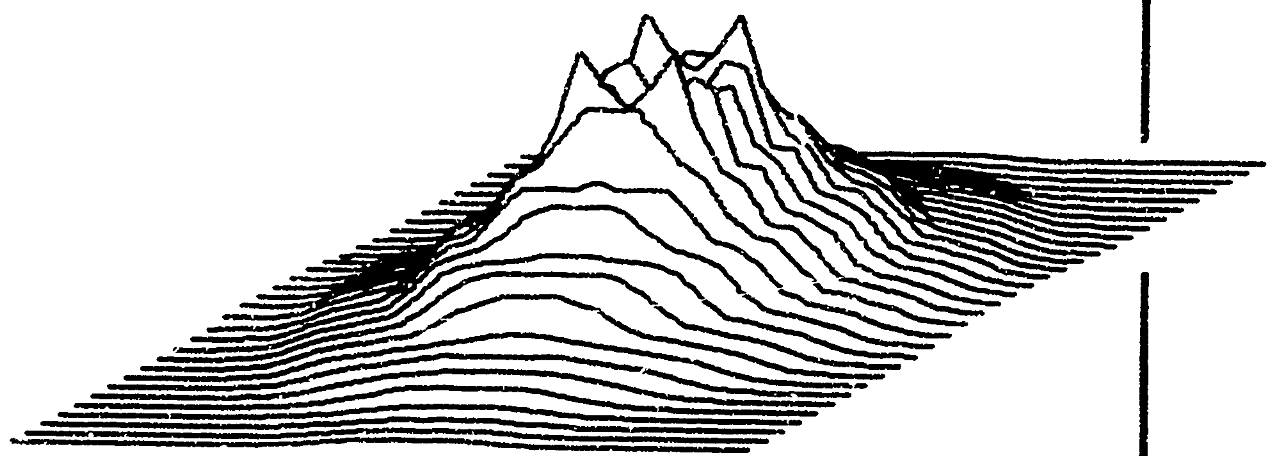

FIGURE 1

THREE-DIMENSIONAL DISPLAY OF RECONSTRUCTED SPHERE

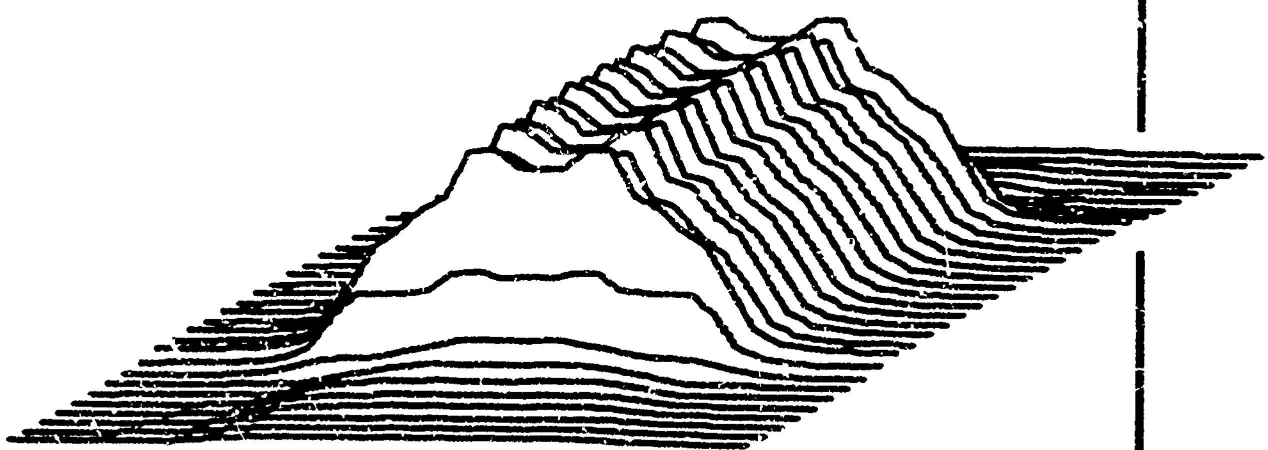

FIGURE 2

THREE-DIMENSIONAL DISPLAY OF RECONSTRUCTED CYLINDER

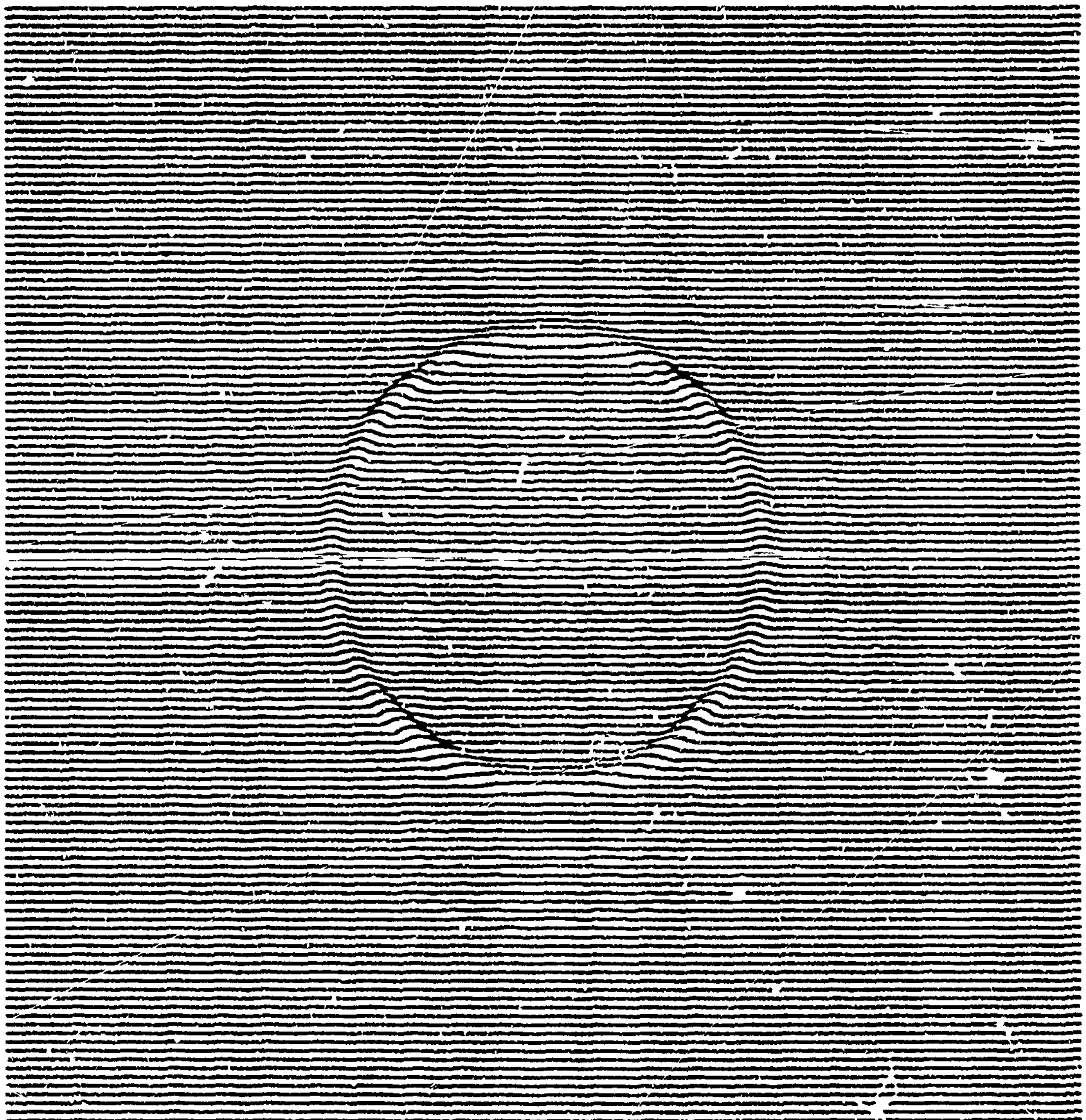

FIGURE 3

TWO-DIMENSIONAL DISPLAY OF RECONSTRUCTED SPHERE FROM SYNTHETIC SCATTERING DATA

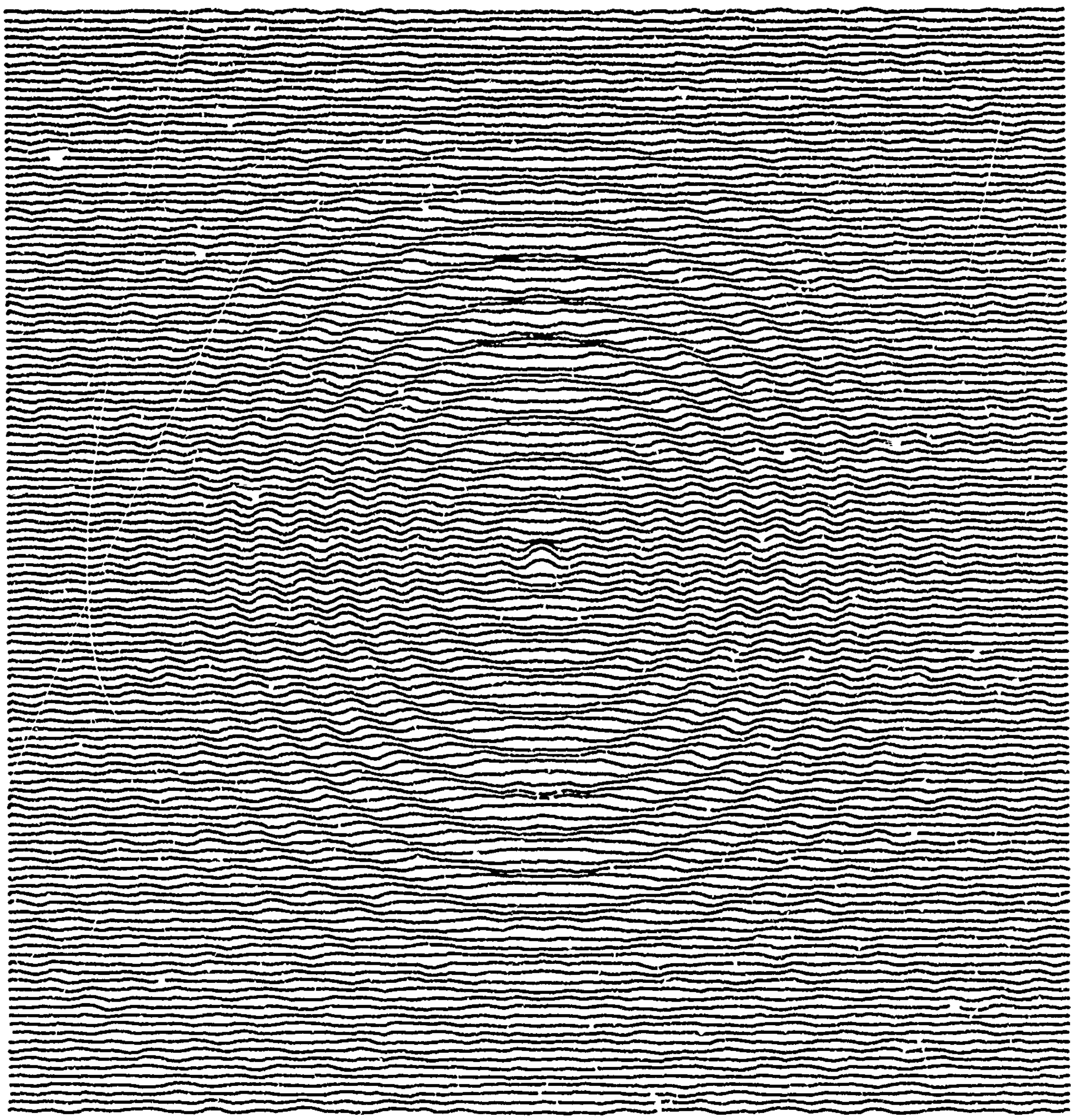

FIGURE 4

TWO-DIMENSIONAL DISPLAY OF RECONSTRUCTED SPHERE FROM MEASURED SCATTERING DATA

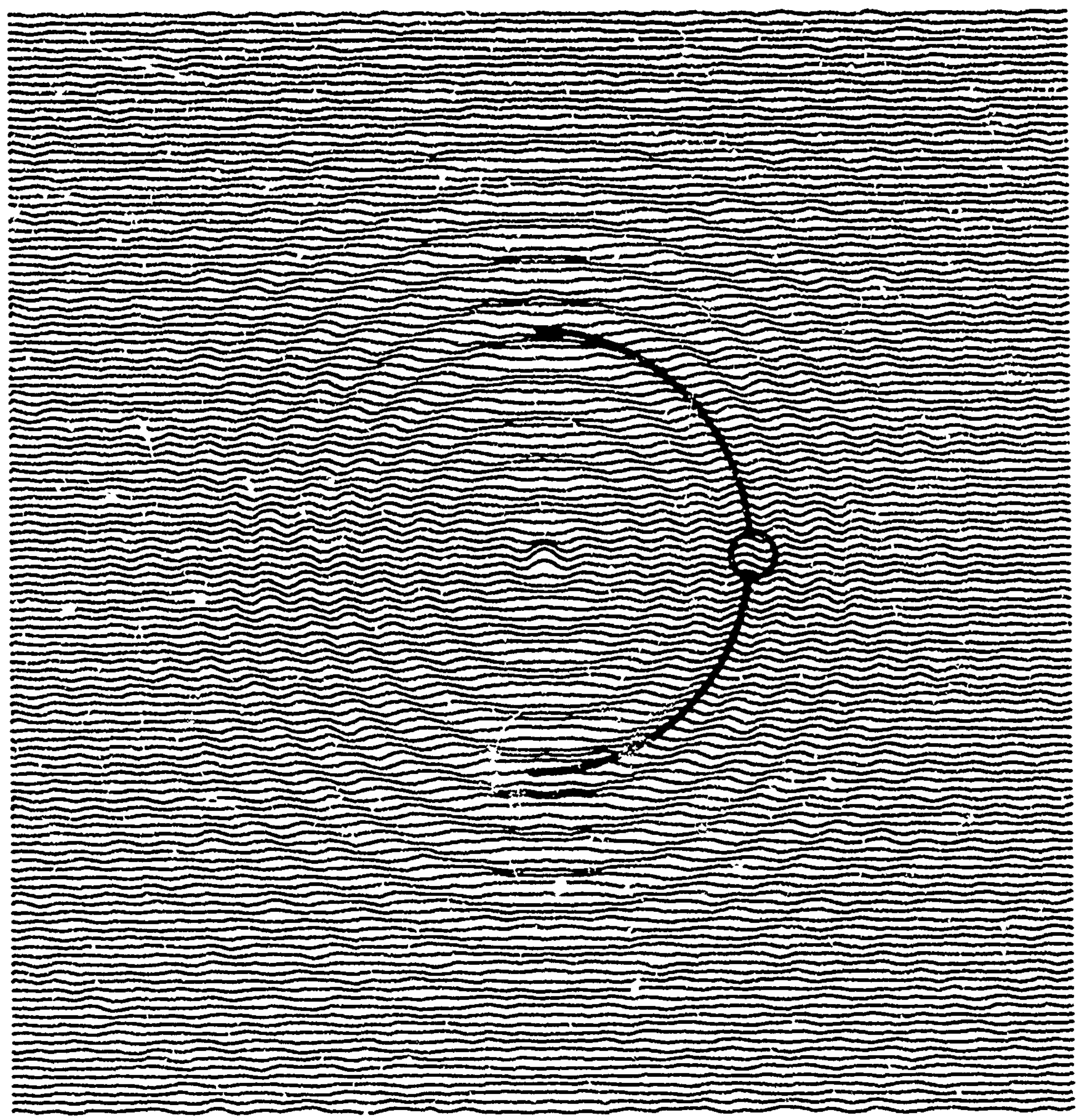

FIGURE 5

TWO-DIMENSINAL D'SPLAY CF RECONSTRUCTED SPHERE FROM MEASURED SCATTERING DATA

SECTION III

EXACT INVERSE SCATTERING

III.1. THEORETICAL RESULTS

The basic Exact Monochromatic Scalar Field Inverse Scattering Integral Equation [14], applicable to complete perspective information, is

$$\int_V dv\, Im\, G\, \rho = \frac{1}{2i} \oint_S d\mathbf{S} \cdot (G^* \nabla\phi - \phi \nabla G^*) \tag{7}$$

which, when ϕ is measured in the far-field, reduces to

$$\int_V dv\, Im\, G\, \rho = \int_{4\pi} d\Omega\, e^{-ik_s \cdot x}\, k_s\, \psi(k_s) \tag{8}$$

where ψ is the range and phase normalized scattered far-field.

For the incomplete perspective information aperture, (8) reduces to the following Double Fredholm Convolution Integral Equation of the First Kind

$$a(x) * Im\, G(x) * \rho(x) = \int_A d\Omega\, e^{-ik_s \cdot x}\, k_s\, \psi(k_s) \tag{9}$$

The time-domain integral equation associated with (7) is

$$\theta(X,t) = \frac{1}{2i}\int_V d^3x' \frac{\rho(X,t-r/c)}{4\pi r} - \frac{1}{2i}\int_V d^3x' \frac{\rho(X,t+r/c)}{4\pi r} \tag{10}$$

The basic equations (7), (8), and (9) are Fredholm Convolution Integral Equations of the First Kind, similar to (3), and can be solved by the methods mentioned in the paragraph subsequent to (3). This author's solution [15] to this integral equation is

$$\boxed{\rho_{n+1}(X) = \rho_n(X) - \frac{1}{\lambda(X)}\int_{V_o} d^3x' \; Im \; G(X|X') \; \rho_n(X') + \frac{\theta(X)}{\lambda(X)}} \tag{11.1}$$

$$\theta \equiv \frac{1}{2i}\oint_S dS\cdot(G^* \nabla\phi - \phi \nabla G^*) \tag{11.2}$$

Preliminary investigations of the time-domain integral equation (10) have been initiated by Prof. N. Bleistein [16].

For the electromagnetic vector fields, equations (7) through (11) have the following respective analogue

$$\int_V d^3x' \; Im \; \nabla G(X|X')\times J(X') = \theta(X) \tag{12}$$

$$\theta \equiv \frac{1}{2i}\oint_S ds \; [\; \nabla G^*\times(n\times H) - \nabla G^*(n\cdot H) + i\omega\varepsilon \; G^*(n\times E) \;] \tag{13}$$

III.2. NUMERICO-EXPERIMENTAL RESULTS

Figure 6 shows the first iteration synthetic computer reconstruction (computer and programmer provided by Dr. G. Tricoles, General Dynamics Corp., San Diego, California) of the source distribution (current) in a half-wave dipole antenna, as per (11). Since the errors are reduced by a factor of two per iteration, an order of ten iterations should suffice for most practical problems. It should be noted, however, that the first iteration already yields reconstruction of the source distribution beyond the Classical Rayleigh Diffraction resolution limit.

Figure 7 and 8 show similar results for the 8^{th}, 16^{th}, and 32^{nd} iterations for a point source, and two point sources one-half wavelengh apart, respectivelly.

FIGURE 6

RECONSTRUCTED HALF-WAVE DIPOLE ANTENNA

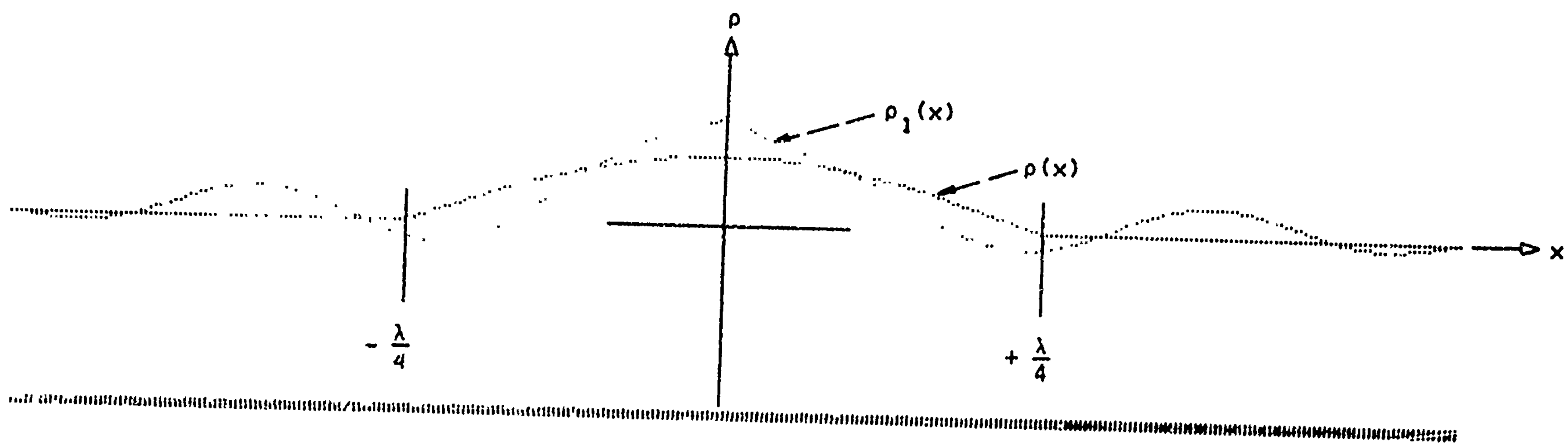

$\rho(x)$ *True* Source Distribution (Half-wave dipole antenna current).

$\rho_1(x)$ First iteration *Reconstructed* (beyond classical Rayleigh diffraction resolution limit) source distribution.

$$\rho(x) = \begin{cases} \cos(kx_1)\,\delta(x_2)\,\delta(x_3) & , \quad x_1 \in (-\frac{\lambda}{4}, +\frac{\lambda}{4}) \\ 0 & , \quad x_1 \notin (-\frac{\lambda}{4}, +\frac{\lambda}{4}) \end{cases}$$

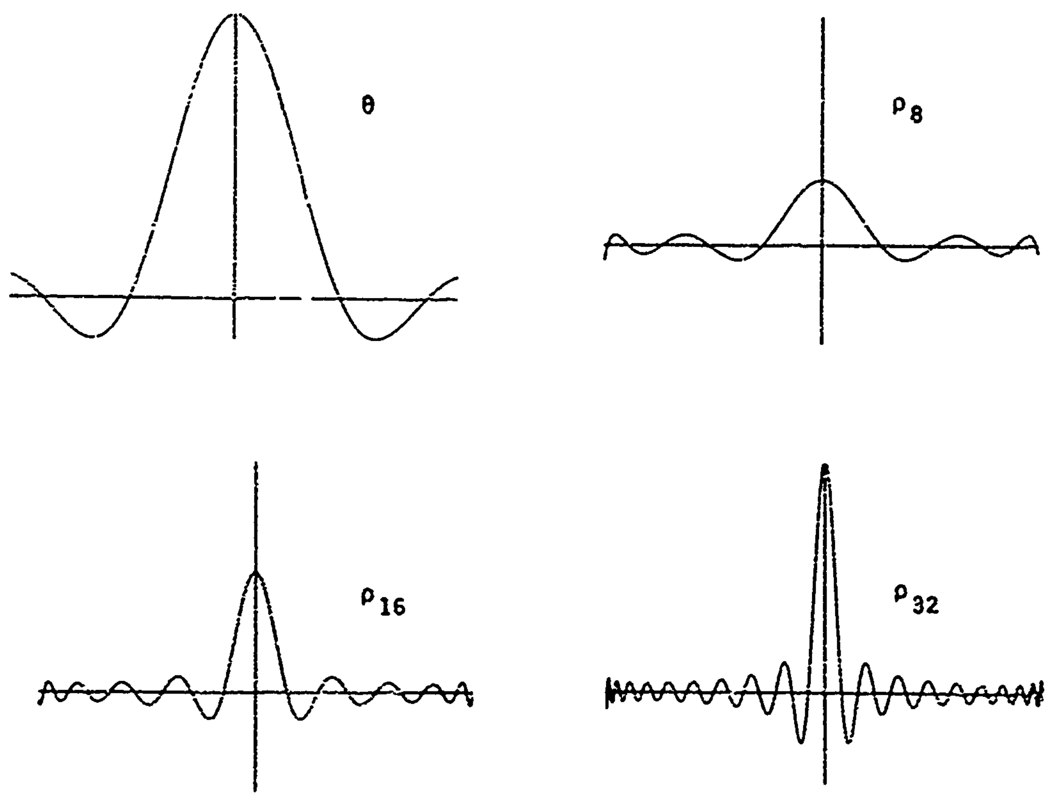

FIGURE 7

RECONSTRUCTED POINT SOURCE

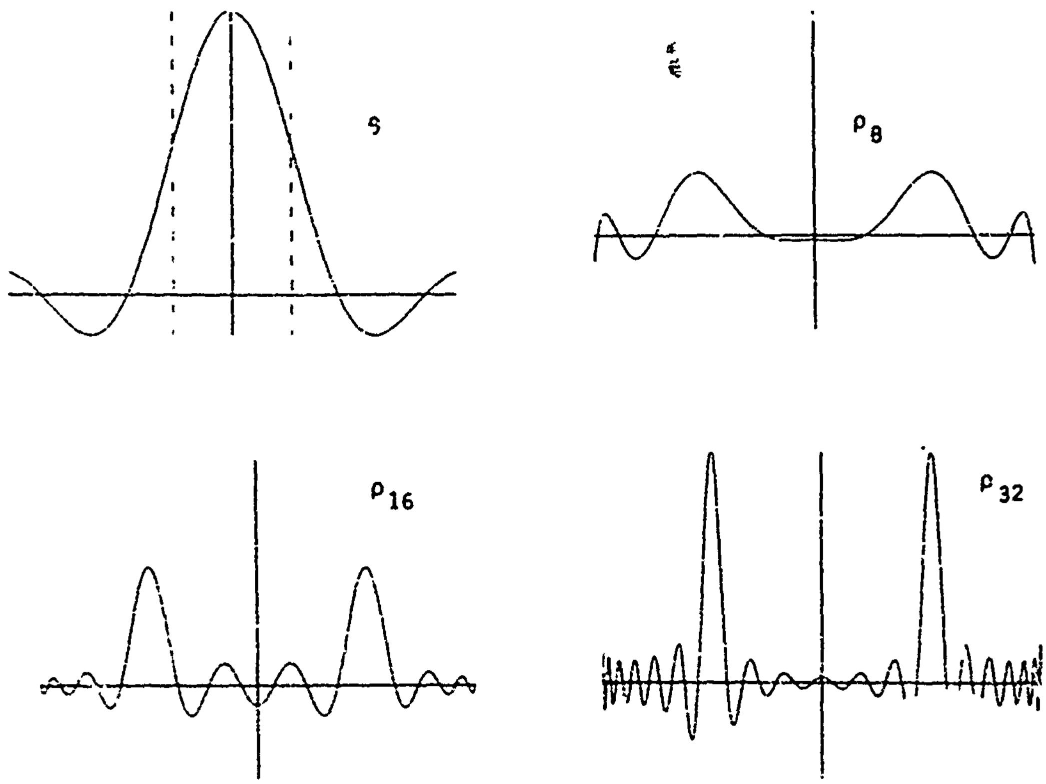

FIGURE 8

RECONSTRUCTED POINT-SOURCE-PAIR

SECTION IV

REFERENCES

[1] Bojarski, N. N., *Inverse Scattering*, Company Report N00019-72-C-0462/F, April 1973, Moorestown, New Jersey 08057.

[2] Bojarski, N. N., *Inverse Scattering*, Company Report N00019-73-C-0312/3, October 1973, Moorestown, New Jersey 08057.

[3] Bojarski, N. N., *k-Space Formulation of the Electromagnetic Scattering Problem*, Company Report F33615-71-C-1576/F, September 1972, Moorestown, New Jersey 08057.

[4] Bojarski, N. N., *Op. Cit. Ref. (1)*, Sect. III, pp. 9-11.

[5] *Ibid*, Sect. IV, pp. 13-15.

[6] Hildebrand, F. B., *Methods of Applied Mathematics*, Sect. 3.18, p. 286, Prentice-Hall, 1965.

[7] *Ibid*, Sect. 3.19, pp. 286-292.

[8] Harrington, R. F., *Field Computation by Moment Methods*, Macmillan, 1968.

[9] Wolf, E., *Progress in Optics*, Vol. VIII, Sect. 6, pp. 39-44, North-Holland, 1970.

[10] Bojarski, N. N., *Op. Cit. Ref. (3)*.

[11] Lewis, R. M., "Physical Optics Inverse Diffraction", *IEEE Transactions on Antennas and Propagation*, Vol. AP-17, No. 3, pp. 308-313, May 1969.

[12] Bojarski, N. N., *Op. Cit. Ref. (1)*, Sect. V, pp. 17-21.

[13] Lewis, R. M., *Op. Cit.*

[14] Bojarski, N. N., *Op. Cit. Ref. (2)*, Sect. II, pp. 3-6.

[15] Bojarski, N. N., *Op. Cit. Ref. (3)*.

[16] Bleistein, N., *Personal Communication*, Dept. of Applied Mathematics, University of Denver, Denver, Colorado.